**Climate
of the Past**

Open Access

Discussions

Sporopollen evidence for Late Miocene stepwise aridification on the Northeastern Tibetan Plateau

J. Liu[1], J. J. Li[1], C. H. Song[2], H. Yu[1], T. J. Peng[1], Z. C. Hui[1], and X. Y. Ye[1]

[1]MOE Key Laboratory of Western China's Environmental Systems & College of Earth and Environmental Sciences, Lanzhou University, Lanzhou 730000, China
[2]Key Laboratory of Western China's Mineral Resources of Gansu Province & School of Earth Sciences, Lanzhou University, Lanzhou 730000, China

Correspondence to: J. J. Li (lijj@lzu.edu.cn)

Discussion Paper | Discussion Paper | Discussion Paper | Discussion Paper

CPD

11, 5243–5268, 2015

Sporopollen evidence for Late Miocene stepwise aridification

J. Liu et al.

Title Page

Abstract	Introduction
Conclusions	References
Tables	Figures

|◀ ▶|

◀ ▶

Back Close

Full Screen / Esc

Printer-friendly Version

Interactive Discussion

Abstract

Holding a climatically and geologically key position both regionally and globally, the northeastern Tibetan Plateau provides a natural laboratory for understanding the interactions between tectonic activity and the evolution of Asian aridification. Determining when and how the Late Miocene climate evolved on the northeastern Tibetan Plateau may help us understand better relations between tectonic uplift, global cooling and ecosystem evolution. Previous paleoenvironmental research has focused on the western Longzhong Basin. Late Miocene aridification data derived from ~~sporo~~pollen now requires corroborative evidence from the eastern Longzhong Basin. Here, we present a Late Miocene ~~sporo~~pollen record from the Tianshui Basin in the eastern Longzhong Basin. Our results show a two-stage stepwise aridification: a temperate forest with a more humid climate developed in the basin between 11.4 and 10.1 Ma, followed by a temperate open forest environment with a less humid climate between 10.1 and 7.4 Ma; and an open temperate forest-steppe environment with a relatively arid climate occupied the basin during 7.4 to 6.4 Ma. The vegetation succession demonstrates that Asian aridification occurred after ~ 7–8 Ma, which is confirmed by other evidence from Asia. Furthermore, this persistent aridification on the northeastern Tibetan Plateau parallels the global cooling of the Late Miocene; the stepwise vegetation succession is consistent with the major uplift of the northeastern Tibetan Plateau during this time. These integrated environmental proxies indicate that global cooling may have been a potential driving force for Asian interior aridification, most likely enhanced by stepwise uplift of the Tibetan Plateau.

1   Introduction

As the latter stage of the global Cenozoic cooling, the Neogene was a critical period for northern hemispheric aridification, especially the marked aridification of the Asian interior. As the world's largest arid region in a temperate zone, it not only provides dust

material for the Chinese Loess Plateau (CLP), but also influences modern Asian so-cial development. Establishing when, and how, this process of aridification began and evolved is therefore vital for elucidating the interactions between tectonic uplift, global cooling and ecosystem evolution. Although there is compelling evidence for the arid-

5 ification of the Asian interior, there is no consensus vis à vis its evolution and driving mechanisms. For instance, previous researchers have suggested that aridification of the Asian interior began in the Late Miocene, based particularly on biological and iso-topic evidence (Eronen et al., 2012; Andersson and Werdelin, 2005; Wang and Deng, 2005; Zhang et al., 2012; Quade et al., 1989; Dettman et al., 2001; Cerling et al., 1997).

10 However, others have argued that the process of Asian aridification may have begun in the Early Miocene (22 Ma) or even earlier (in the Late Oligocene), as inferred from Miocene or Oligocene eolian deposition (Guo et al., 2002, 2008; Qiang et al., 2011; Sun et al., 2010). The particular driving mechanisms of such aridification also remain enigmatic. Up until now, the tectonic uplift of the Tibetan Plateau (TP), global cooling,

15 polar ice-sheet volumes and land–sea distributions etc. have been suggested as the major drivers (Kutzbach et al., 1993; An et al., 2001; Liu and Yin, 2002; Molnar et al., 2010; Gupta et al., 2004; Miao et al., 2012). However, the question of which one of these has principally controlled Asian climatic evolution is far from agreed. We focused on an ideal region – the northeastern TP – to explore the nature of the interactions

20 between tectonics and the climate.

The geographically-extensive Longzhong Basin, consisting of series sub-basins, is located in the northeastern TP. These sub-basins present a continuous record of mam-malian fossil-rich Cenozoic sediments, recording the effect of TP uplift on regional cli-mates (GRGST, 1984; Fang et al., 2003, 2005; Li et al., 2006, 2014). On the other

25 hand, it lies in the so-called monsoonal triangle zone, a transition zone from a warm-humid Asian monsoonal climate, to a dry-cold inland climate, to the alpine climate of the TP (Li et al., 1988, 2014) (Fig. 1a). Its particular geological and geographical char-acteristics make it sensitive to the accurate recording of the aridification of northern China through and the evolution of the Asian Monsoon. As an ideal field laboratory for

studying tectonic-climate interactions (Molnar et al., 2010; Tapponnier et al., 2001), the Longzhong Basin region might be the most promising for distinguishing TP uplift and ~~any~~ associated environmental change.

As a reliable paleoenvironmental proxy, ~~sporo~~pollen has been used to reconstruct
5   past climates because of its abundance and excellent preservation within sediments. Previous research has demonstrated that the Tianshui Basin, as a sub-basin of the Longzhong Basin, exhibits a typical Late Miocene lacustrine-fluvial sedimentary succession containing abundant pollen~~s~~. Here we reconstruct a high-resolution palynological record from the well-dated Yaodian Section, located in the southern part of the
10   Tianshui Basin. Our results not only provide new evidence for the evolution of vegetation in the Late Miocene and climate change on the northeastern margins of the TP, but also shed new light on the aridification of the Asian interior through time. We also discuss the possible relation between tectonic activity and climate change.

2   Geological and geographical settings

15   The rhomboid-shaped Longzhong Basin, which is one of the largest intermountain and fault-controlled sedimentary basins on the northeastern TP, is geographically delineated by the left-lateral strike-slip Haiyuan Fault to the north, the Liupan Shan Fault to the east and northeast, the Laji Shan Fault to the southwest, and the Western Qinling Fault to the south (Fig. 1b). The Tianshui Basin, one of its sub-basins, is located in
20   the southeastern part of the Longzhong Basin (Fig. 1b). It has witnessed the continuous deposition of mammalian, fossil-rich Cenozoic sediments from the surrounding mountains; these sediments record the interactions between mountain uplift, erosion and climate change (Li et al., 2006; Alonso-Zarza et al., 2009; Peng et al., 2012). At present, the East Asian Monsoon influences this region, engendering a semi-humid,
25   warm temperate, continental monsoon climate, characterized by relatively hot, humid summers and cold, dry winters. The mean annual temperature and mean annual precipitation of this area are $\sim 10.4\,°C$ and $504\,mm$, respectively, with rainfall concentrated

mainly in ~~the~~ summer and autumn (Fig. 1c). The modern natural vegetation in this region is warm-temperature forest-grassland. Warm grasslands are distributed in the valleys, and consist mainly of *Arundinella hirta*, *Spodiopogon sibiricus* and *Themeda triandran*. Shrubs such as *Zizyphus jujube*, *Sophora viciifolia* and *Ostryopsis davidiana*
5 are found on the hillsides. Trees, including *Quercus liaotungensis*, *Pinus tabulaeformis*, *P. armandi* and *Platycladus orientalis*, grow in the mountains (Huang, 1997).

The selected Yaodian Section (105°55′ E, 34°38′ N) is located in the southern part of the Tianshui Basin (Fig. 1d). The Neogene sequence in this section is capped by Quaternary loess and lies unconformably on top of the Paleogene Guyuan Group. It has
10 been divided into the Ganquan Formation (Fm), the Yaodian Fm and the Yangjizhai Fm, in sequence upwards (Li et al., 2006). In this study, our research mainly focuses on the Late Miocene Yaodian Fm and Yangjizhai Fm. Based on a determination of lithology and sedimentology, the Yaodian Fm can be divided into three principal strata. The lower stratum consists of massive fine gravel sandstone, sandstone and brown silty mud-
15 stone, occasionally with thin brown mudstone or interbedded paleosols, which can be considered fluvial channel deposits (Fig. 2e). Abundant teeth of *Hipparion weihoense*, *Cervavitus novorossiae*, *Ictitherium* sp. and their bone fragments were excavated from this stratum. The middle stratum of the Yaodian Fm consists of the interbedding of siltstone or fine sandstone with mudstone intercalated with paleosols, overlying the fluvial
20 channel deposits. This assemblage's characteristics are typical of floodplain deposition (Fig. 2d). The upper stratum of the Yaodian Fm is characterized by rhythmic cycles composed of grey or brown mudstone or sandy marlite and intraclastic marl intercalated with brown siltstone and mudstone, and contains fossil algae and gastropods; this section is representative of shallow lake deposition (Fig. 2a and c). This upper
25 stratum is common throughout the basin, and is analogous to the "Zebra Bed" stratum found in the Linxia Basin in the western Longzhong Basin (Li, 1995). The Yangjizhai Fm is principally composed of reddish brown mudstone or silty mudstone and yellow-brown calcrete or calcareous mudstone, with scattered sandstone or grey mudstone and marlite. These sediments were deposited under strong evaporative conditions in

distal floodplain to palustrine environments (Fig. 2b). Previous paleomagnetic investigations have indicated that the Yaodian Fm ranges from 11.67 to 7.43 Ma in age, and that the Yangjizhai Fm dates from 7.43 to 6.40 Ma, both these ranges being consistent with the formations' biostratigraphic ages (Li et al., 2006).

3   Materials and methods

Most of the samples came from lacustrine mud deposits and fine grain size intercalations found in floodplain and fluvial channel deposits. Because the lower 10 m of the Yaodian Fm consists of coarse gravel sandstone, and it was difficult to find fine-grained sediments therein, this part of the formation was not sampled. A total of 200 samples were processed for ~~sporopollen~~ analysis. For each sample, > 100 g of sediment was washed in 20 % HCl, soaked in 39 % HF and then treated with 10 % HCl solution to enable fluoride dissolution. The chemical processing was followed by physical enrichment procedures ~~such as~~ ZnCl$_2$ separation, ultrasound sieving ~~with~~ a 10 µm filter, ~~and storage~~ in glycerin. ~~Sporopollen grains~~ were identified by ~~comparing samples with published modern and fossil sporopollen plates (~~Wang, 1995; Song, 1999), as well as modern ~~sporopollen~~ slides ~~preserved in~~ the Laboratory of Sporopollen Analysis of the Geography Department of Lanzhou University.

4   Results

Only 126 of the 200 samples contained enough palynomorphs to provide reliable data; the remaining 74 possessed fewer than 300 identifiable grains. Most of the~~se~~ latter samples had been preserved under oxidizing conditions, or had ~~abundant~~ carbonate content. Approximately 80 different palynomorphs were identified ~~into~~ family or genus. ~~In order to synthesize the information and highlight palynological trends, the major taxa, and their percentage contents vis-à-vis recognized taxa, were used to construct a sporopollen diagram~~ (Fig. 3).

This diagram principally demonstrates that tree pollen declines stepwise as herbaceous pollen increases. Tree pollen consists mainly of *Pinus*, Cupressaceae and *Ulmus*, along with *Quercus* and *Betula*. Additionally, a number of subtropical plants such as *Liquidambar*, *Pterocarya*, *Carya* and Euphorbiaceae (which is no longer found in this area today), appear often, but their contents are lower. Herbaceous pollen is mainly from *Artemisia*, Chenopodioideae, Poaceae and Asteraceae. Pollen from extremely drought-tolerant plants, such as *Ephedra* and *Nitraria*, only appear sporadically in individual samples. In addition, this section also contains some ferns and *Pediastrum*. Stratigraphically-constrained cluster analysis (CONISS) yields three distinct zones in the section, described from the bottom up as follows:

4.1 Zone 1 (13.1–10.1 Ma)

Samples from this zone exhibit high percentages of tree pollen (averaging 75.13 %) and relatively less herbaceous pollen (averaging 23.42 %). Coniferous taxa are mainly *Pinus* (18.57 %) and Cupressaceae (17.62 %), with smaller amounts of *Picea* and *Cedrus*. *Ulmus* (19.71 %) is the most common broadleaf tree, accompanied by *Betula* (2.73 %), *Quercus* (2.17 %) and *Salix* (2.10 %). Other arboreal taxa are *Juglans* and *Castanea*, with < 2 % each. Herbaceous taxa mainly include *Artemisia* (7.41 %), Chenopodioideae (5.51 %) and Poaceae (2.44 %), along with small amounts of Asteraceae, Ranunculaceae and Rosaceae, with amounts < 2 % each. Aquatic plants, algae and some subtropical taxa are also present in this zone, though with low contents.

4.2 Zone 2 (10.1–7.4 Ma)

In samples from this zone, total tree pollen content decreases, averaging 53.98 %, while the percentage of herbaceous pollen (averaging 42.93 %) increases. Coniferous taxa are principally represented by *Pinus* (13.95 %), Cupressaceae (7.48 %), *Picea* (2.16 %) and *Cedrus* (1.49 %). Among broadleaf trees, the dominant taxa are *Ulmus* (averaging 8.04 %), *Quercus* (2.35 %), *Betula* (2.28 %), *Salix* (1.89 %) and *Juglans*

(1.42 %). Herbaceous taxa are dominated by *Artemisia* (13.68 %) and Chenopodi-oideae (8.83 %), along with Poaceae (4.89 %), Asteraceae (3.15 %) and Ranuncu-laceae (2.94 %). Aquatic vegetation ~~appears successively and~~ reaches the highest value found in the entire profile. ~~There are also some~~ subtropical taxa with ~~low con-tents~~, such as *Liquidambar*, *Pterocarya*, *Carya* and Rutaceae. This zone is divided into two subzones, Zone 2-1 (10.1–8.6 Ma) and Zone 2-2 (8.6–7.4 Ma). Herbaceous pollen percentages are slightly higher in Zone 2-2 than in Zone 2-1.

4.3 Zone 3 (7.4–6.4 Ma)

The samples from this zone record a ~~sudden~~ decrease in tree pollen ~~(with content av-eraging 39.20 %), mirrored by an increase in herbaceous pollen (averaging 60.08 %)~~. Coniferous taxa are characterized by *Pinus* (7.24 %) and Cupressaceae (5.26 %). *Ul-mus* (5.28 %) dominates the broadleaf tree ~~category~~, with *Quercus* and *Betula* account-ing for 2.33 and 2.32 %, respectively. Herbaceous taxa are composed of *Artemisia* (19.42 %), Chenopodioideae (11.23 %) and Poaceae (8.59 %), together with Aster-aceae (4.53 %), Ranunculaceae (3.23 %), Brassicaceae (3.18 %) and Polygonaceae (1.86 %). Aquatic plants and thermophilic species almost disappear.

5 Discussion

5.1 Vegetation and climate reconstruction

~~When discussing the relation between the palynological spectrum and sedimentary fa-cies in the Yaodian Section, it becomes apparent that these~~ sedimentary facies ~~have experienced~~ four successive depositional stages: fluvial channel; floodplain; shallow lake; and distal floodplain to palustrine. Transition~~al ages~~ can be dated to 10.4, 9.23 and 7.43 Ma, respectively (Li et al., 2006) (Fig. 2). Our palynological ~~spectrum~~ shows stepwise changes at 10.1 and 7.4 Ma, lagging slightly behind those evinced by the sedimentary facies. Another distinctive feature of the palynological ~~spectrum~~ is that the

green lacustrine deposits of fine grain size exhibit dense palynomorph concentrations, with higher tree pollen percentages. In contrast, the reddish floodplain deposits with coarse grain sizes possess sparse palynomorph concentrations, with higher herbaceous pollen percentages (Fig. 3). However, in the same ~~sporo~~pollen zones, we find that the palynomorph concentration clearly changes between different sedimentary facies, but that ~~any variation in overall~~ percentage ~~content is~~ minor. ~~Interestingly,~~ between different sporopollen zones, the palynomorph percentage changes ~~greatly vis à vis~~ the same sedimentary facies. We can therefore conclude that the~~se~~ changes in the palynological ~~spectrum~~ are caused by changes in regional vegetation, rather than differ~~ing~~ preservation conditions. The paleoecological information inferred from the percentage change of sporopollen record can thus be considered reliable.

According to modern surface pollen studies, *Pinus* is often overrepresented in pollen records because of its abundant pollen production and the ease with which this pollen is transported over long distances by ~~the~~ wind. As a general rule, it can be assumed that there is/was no proximate pine forest if less than 25 to 30 % of *Pinus* pollen occurs in samples (Li and Yao, 1990). Higher percentages of Cupressaceae and Taxodiaceae coexistent with temperate tree, shrub and herbaceous pollen may reflect a warmer, wetter and more humid climate (Song, 1978). Nowadays, *Ulmus* is commonly distributed in the sub-humid temperate and warm temperate mountain foothills of northern China, but percentages of its pollen collected from CLP surface soils never exceed 1 %, even under broadleaved forests containing elm (Liu et al., 1999). In general, when their ~~content~~ exceeds 3–5 % of ~~total~~ arboreal pollen ~~content,~~ birch and oak can be considered to be/have been present in woodland (Liu et al., 1999). *Salix* produces very little pollen, and most of this pollen falls near the tree itself (Li et al., 2000). Modern *Artemisia* and Chenopodioideae are extensively distributed throughout the arid and semi-arid regions of China. Chenopodioideae are more drought-resistant than *Artemisia*. *Artemisia* ~~being the dominant vegetation type~~ may reflect a semi-arid grassland environment, while Chenopodioideae may reflect an arid desert environment. Surface pollen analysis shows that *Artemisia* and Chenopodioideae are greatly overrepresented in pollen

Title Page

Abstract | Introduction

Conclusions | References

Tables | Figures

|◀ | ▶|

◀ | ▶

Back | Close

Full Screen / Esc

Printer-friendly Version

Interactive Discussion

rain. Only when Chenopodioideae and *Artemisia* pollen ~~content~~ exceeds 30 % of the total should their presence be considered as primarily local (Herzschuh et al., 2003; Ma et al., 2008). Poaceae pollen ~~content~~ is sparse, usually only 3–6 %, even when it represents the dominant modern species (Tong et al., 1995).

5　　Our record therefore indicates that, during the period when the Yaodian Fm was being deposited, the study area was ~~dominated~~ by temperate forests and a warm and humid climate. Mixed deciduous forests, characterized by the dominance of *Pinus*, Cupressaceae, *Ulmus* and *Quercus*, were distributed within the basin and the low altitude hills surrounding it. Mid- and high-altitude ~~vegetation, such as~~ *Abies*, *Picea and Cedrus*,

10 existed in the surrounding uplands. The river banks or lake margins were colonized by *Salix*, *Alnus*, *Fraxinus* and Taxodiaceae. Cyperaceae, *Typha* and *Myriophyllum* grew along the lake shores or in shallow water areas. Ranunculaceae, Poaceae, Chenopodioideae and *Artemisia*, principally occupied the forest understory, or were distributed in forest clearings. However, as indicated by our record, the environment was not static.

15 During 11.4–10.1 Ma, temperate forest ~~and~~ a ~~more~~ humid climate ~~developed in the basin~~. The growth of fluvial channel deposits and the presentation of a large number of mammalian fossils (Li et al., 2006) also support the theory that much denser vegetation capable of supporting large mammals such as rhinoceroses developed during this interval. Moreover, we know that the northern Tianshui Basin was dominated by

20 temperate and warm-temperate deciduous broadleaf forest (Hui et al., 2011). Our result is also consistent with research into the climatic evolution of the Qaidam Basin, which found that the presence of δ^{18}O values characteristic of large mammals indicated a warmer, wetter, and perhaps lower-altitude Qaidam Basin (Zhang et al., 2012). The early Late Miocene mammal fauna discovered in the Qaidam Basin also reflected

25 a wooded environment, in which many streams with aquatic plants such as *Trapa* and *Typha* developed (Wang et al., 2007). From 10.1–7.4 Ma, the study area was dominated by a warm-temperate open forest environment and ~~an~~ arid climate, relative to the previous interval. Sedimentary facies become characteristic of shallow lake deposits (Li et al., 2006). Mammal fauna identified in the eastern Qaidam Basin also indicate that

Sporopollen evidence for Late Miocene stepwise aridification

J. Liu et al.

a mixed habitat of open and wooded environments, with abundant freshwater streams, was predominant at that time (Wang et al., 2007). During this interval, after ~ 8.6 Ma, herbaceous plants also increased their presence in the Tianshui Basin, as confirmed by mammalian fossil records. In the northern Tianshui Basin at ~ 9.5 Ma, there is evidence
5 of a sizeable rhinoceros population, which would have required a relatively moist woodland environment to sustain itself. However, the typical *Hipparion* fauna that presents ~ 8.0 Ma probably represents a relatively temperate climate with a more mixed vegetative landscape, i.e. an open forest environment rather than a vast, open landscape. Large mammals would still have been able to survive in such an environment (Zhang
10 et al., 2013).

An open temperate forest-steppe environment clearly developed in the study region, indicating significant aridification after ~ 7.4 Ma. Grassland, composed principally of Poaceae, *Artemisia* and Chenopodioideae, developed in most of the basin, while shrinking areas of open forest, dominated by Cupressaceae, *Ulmus* and *Quercus*, ex-
15 isted in the surrounding mountains. *Salix* continued to grow in relatively humid environments such as riverbanks. Distal floodplain to palustrine deposits now characterize the study area (Li et al., 2006). A sudden increase in magnetic susceptibility after ~ 7.4 Ma may indicate the enhanced oxidation characteristic of an arid environment (Fig. 4b). In the northern part of the Tianshui Basin, drought-tolerant *Artemisia* predominates after
20 7.4 Ma, further confirming the presence of a drier climate (Hui et al., 2011) (Fig. 4c). Further, the growing presence of grazer mammalian species at the end of the Miocene in the Tianshui Basin suggests that the local environment was principally occupied by grassland, with some woodland, and even some desertification (L. P. Liu et al., 2011) (Fig. 4d). Furthermore, the gradual increase in eolian sediments after 7.4 Ma in the
25 Linxia Basin would indicate a period of intense desertification in central China (Fan et al., 2006) (Fig. 4e). Biomarker evidence from the Linxia Basin also indicates a distinct change in the climate toward arid-cold conditions at ~ 8 Ma (Wang et al., 2012). The isotopic compositions of herbivorous fossil teeth and paleosols from the Linxia Basin (Wang and Deng, 2005) and southwestern China (Biasatti et al., 2012) also

indicate a shift to a drier, or seasonally drier, local climate. In the Qaidam Basin, *Hipparion teilhardi* fossils characterized by slenderer distal limbs, and dated to the end of the Miocene, imply an adaptation by this animal to the open steppe environment (Deng and Wang, 2004). Marine sediments also indicate that the climate changed at this time.

5 For example, local seawater δ^{18}O reconstructions from ODP Site 1146 in the northern South China Sea suggest that the climate of East and South Asia shifted toward more arid conditions after ~ 7.5 Ma (Steinke et al., 2010) (Fig. 4f).

5.2 More arid conditions at the end of the Miocene and their possible causes

Based on the currently-available data from Late Neogene Chinese mammalian fos-
10 sils, Zhang (2006) suggested that mammal communities in northern China were rather stable and uniform from ~ 13 Ma to the end of the Miocene (~ 7–8 Ma), and that differentiation between the humid fauna communities prevalent in eastern China and the dry fauna communities identified in western China occurred after the end of the Miocene. The diversity in Bovidae fossils also increases significantly toward the end of the
15 Miocene, with some genera ~~even~~ appearing in southwestern China (Chen and Zhang, 2009), indicating an expansion in grasslands and ~~an~~ aridification ~~of the climate~~. Using macro- and microfloral quantitative recovery techniques to reconstruct the climate in northern China at the time, Y.-S. C. Liu et al. (2011) proposed that the west–east temperature and precipitation gradient pattern did not develop in northern China until the
20 end of the Miocene. This corroborates the quantitative results gained from using mammalian fossils as a proxy for paleoprecipitation (Liu et al., 2009). A semi-quantitative reconstruction of Chinese Neogene vegetation also indicates that the aridification of western, central and northern China occurred during the Miocene–Pliocene transition (Jacques et al., 2013). Indeed, in order to adapt to the arid climate in northern China
25 during the end of the Miocene, some plants and arthropods also evolved more arid-tolerant species, such as *Frutescentes* (Fabaceae) (Zhang and Fritsch, 2010), *Ephedra* (Ephedraceae) (Qin et al., 2013) and *Mesobuthus* (Buthidae) (Shi et al., 2013). This marked aridification has been well documented in other parts of Asia. For example,

dramatic changes in the carbon and hydrogen isotopic ratios of leaf waxes at ODP Site 722 indicate an increasing aridity at the end of the Miocene in continental source regions, including Pakistan, Iran, Afghanistan, and the Arabian Peninsula (Huang et al., 2007) (Fig. 4g). The isotopic compositions of herbivorous fossil teeth and paleosol carbonates also suggest that the climate became drier over the Indian Subcontinent, China, and Central Asia during toward the end of the Miocene (Quade et al., 1989; Cerling et al., 1997; Wang and Deng, 2005; Biasatti et al., 2012; Barry et al., 2002; Badgley et al., 2008; Zhang et al., 2009). The evidential synchronicity of these climatic events in Asia strongly suggests that a process of aridification began toward the end of the Miocene (∼ 7–8 Ma). The onset of such a marked aridification is further corroborated by the presence of red clay across much of the CLP (An et al., 2001).

In our study, the vegetation succession appears to be consistent with the general direction of global cooling, indicating that global cooling may have been a potential driving force for the aridification of the Asian interior (Fig. 4h). Because atmospheric moisture content decreases as air temperature cools, one would expect global cooling to lead to a gradual net global aridification (van Dam, 2006). However, drought occurs in a stepwise fashion. Although the most significant Late Cenozoic global cooling event occurred at ∼ 14 Ma (Zachos et al., 2001), only minor cooling events at ∼ 10.1 Ma and ∼ 7.4 Ma have been documented (Fig. 4h). The Late Miocene climate was much warmer and/or wetter than today in many regions (Pound et al., 2012). Evidently, factors other than global cooling also exert a strong effect on precipitation regimes, particularly paleotopography and continental tectonic configuration, which themselves affect monsoonal patterns.

The uplift of the TP is a potentially significant trigger of Asian aridification. First, although no consensus exists vis-à-vis the timing and degree of any uplift, many studies have suggested that the interval ∼ 8–10 Ma not only experienced rapid uplift of the TP (Molnar et al., 2010; Fang et al., 2003, 2005; Li et al., 2014; Enkelmann et al., 2006; Zheng et al., 2006, 2010; Wang et al., 2012, 2006; Lease et al., 2007) (Fig. 4i), but that this uplift achieved an altitude sufficient to block the penetration of moisture from

the Indian Ocean into western China (Dettman et al., 2001, 2003). Second, the main source of water vapor for arid northwestern China has been the Asian Summer Monsoon; the Asian Winter Monsoon promotes a cold and dry climate. Atmospheric and coupled atmosphere–ocean models show that such massive, continent-spanning oro-

5 gen uplift may have generated, or intensified, Asian monsoonal circulation (Kutzbach et al., 1993; An et al., 2001). Moreover, the effect of TP uplift on enhancement of the Asian Winter Monsoon was more significant than on the Asian Summer Monsoon (Liu and Yin, 2002). There is increasing evidence that the Asian Summer Monsoon gradually weakened after ~ 10 Ma (Wan et al., 2010; Clift et al., 2008), while the Asian Winter

10 Monsoon gradually strengthened, particularly toward the end of the Miocene (An et al., 2001; Jacques et al., 2013; Clift et al., 2008; Sun and Wang, 2005; Jia et al., 2003). Therefore, global cooling, most likely enhanced by TP uplift, may be a potential driving force for the aridification of the Asian interior.

6   Conclusion

15 The Late Cenozoic basins in the northeastern TP document both the tectonic uplift process and its associated environmental changes. We investigated a Late Miocene sporopollen record from the Tianshui Basin in the northeastern TP. Our results indicated that a temperate forest, with a more humid climate regime (11.4–10.1 Ma), gave way to a temperate open forest environment with a less humid climate (10.1–7.4 Ma);

20 this was in turn replaced by an open temperate forest-steppe landscape, accompanied by a relatively arid climate (7.4–6.4 Ma). This vegetation succession demonstrates that aridification of the Asian interior occurred after ~ 7–8 Ma, as corroborated by other studies of Asia. Our findings support the idea that global cooling may have been a potential driving force for aridification of the Asian interior, and that TP uplift probably en-

25 hanced this process. This study highlights these possible interactions between global cooling and tectonic uplift.

References

Alonso-Zarza, A. M., Zhao, Z. J., Song, C. H., Li, J. J., Zhang, J., Martín-Pérez, A., Martín-García, R., Wang, X. X., Zhang, Y., and Zhang, M. H.: Mudflat/distal fan and shallow lake sedimentation (upper Vallesian-Turolian) in the Tianshui Basin, Central China: evidence against the late Miocene eolian loess, Sediment. Geol., 222, 42–51, 2009.

An, Z. S., Kutzbach, J. E., Prell, W. L., and Porter, S. C.: Evolution of Asian monsoons and phased uplift of the Himalaya-Tibetan plateau since Late Miocene times, Nature, 411, 62–66, 2001.

Andersson, K. and Werdelin, L.: Carnivora from the late miocene of Lantian, China, Vertebrat. Palasiatic., 43, 256–271, 2005.

Badgley, C., Barry, J. C., Morgan, M. E., Nelson, S. V., Behrensmeyer, A. K., Cerling, T. E., and Pilbeam, D.: Ecological changes in Miocene mammalian record show impact of prolonged climatic forcing, P. Natl. Acad. Sci. USA, 105, 12145–12149, 2008.

Barry, J. C., Morgan, M. E., Flynn, L. J., Pilbeam, D., Behrensmeyer, A. K., Raza, S. M., Khan, I. A., Badgley, C., Hicks, J., and Kelley, J.: Faunal and environmental change in the late Miocene Siwaliks of northern Pakistan, Paleobiology, 28, 1–71, 2002.

Biasatti, D., Wang, Y., Gao, F., Xu, Y. F., and Flynn, L.: Paleoecologies and paleoclimates of late cenozoic mammals from Southwest China: evidence from stable carbon and oxygen isotopes, J. Asian Earth Sci., 44, 48–61, 2012.

Cerling, T. E., Harris, J. M., MacFadden, B. J., Leakey, M. G., Quade, J., Eisenmann, V., and Ehleringer, J. R.: Global vegetation change through the Miocene/Pliocene boundary, Nature, 389, 153–158, 1997.

Chen, G. F. and Zhang, Z. Q.: Taxonomy and evolutionary process of Neogene Bovidae from China, Vertebrat. Palasiatic., 10, 265–281, 2009.

Clift, P. D., Hodges, K. V., Heslop, D., Hannigan, R., Van Long, H., and Calves, G.: Correlation of Himalayan exhumation rates and Asian monsoon intensity, Nat. Geosci., 1, 875–880, 2008.

Deng, T. and Wang, X. M.: Late Miocene *Hipparion* (Equidae, Mammalia) of eastern Qaidam Basin in Qinghai, China, Vertebrat. Palasiatic., 42, 316–333, 2004.

Dettman, D. L., Kohn, M. J., Quade, J., Ryerson, F. J., Ojha, T. P., and Hamidullah, S.: Seasonal stable isotope evidence for a strong Asian monsoon throughout the past 10.7 myr, Geology, 29, 31–34, 2001.

Dettman, D. L., Fang, X. M., Garzione, C. N., and Li, J. J.: Uplift-driven climate change at 12 Ma: a long δ^{18}O record from the NE margin of the Tibetan plateau, Earth Planet. Sc. Lett., 214, 267–277, 2003.

Enkelmann, E., Ratschbacher, L., Jonckheere, R., Nestler, R., Fleischer, M., Gloaguen, R., Hacker, B. R., Zhang, Y. Q., and Ma, Y. S.: Cenozoic exhumation and deformation of northeastern Tibet and the Qinling: is Tibetan lower crustal flow diverging around the Sichuan Basin?, Geol. Soc. Am. Bull., 118, 651–671, 2006.

Eronen, J. T., Fortelius, M., Micheels, A., Portmann, F. T., Puolamäki, K., and Janis, C. M.: Neogene aridification of the Northern Hemisphere, Geology, 40, 823–826, 2012.

Fan, M. J., Song, C. H., Dettman, D. L., Fang, X. M., and Xu, X. H.: Intensification of the Asian winter monsoon after 7.4 Ma: grain-size evidence from the Linxia Basin, northeastern Tibetan Plateau, 13.1 to 4.3 Ma, Earth Planet. Sc. Lett., 248, 186–197, 2006.

Fang, X. M., Garzione, C., Van der Voo, R., Li, J. J., and Fan, M. J.: Flexural subsidence by 29 Ma on the NE edge of Tibet from the magnetostratigraphy of Linxia Basin, China, Earth Planet. Sc. Lett., 210, 545–560, 2003.

Fang, X. M., Yan, M. D., Van der Voo, R., Rea, D. K., Song, C. H., Parés, J. M., Gao, J. P., Nie, J. S., and Dai, S.: Late Cenozoic deformation and uplift of the NE Tibetan Plateau: evidence from high-resolution magnetostratigraphy of the Guide Basin, Qinghai Province, China, Geol. Soc. Am. Bull., 117, 1208–1225, 2005.

Gansu Regional Geological Survey Team (GRGST): The tertiary system of Gansu province, in: Gansu Geology, People's Press of Gansu, Lanzhou, China, 1–40, 1984.

Guo, Z. T., Ruddiman, W. F., Hao, Q. Z., Wu, H. B., Qiao, Y. S., Zhu, R. X., Peng, S. Z., Wei, J. J., Yuan, B. Y., and Liu, T. S.: Onset of Asian desertification by 22 Myr ago inferred from loess deposits in China, Nature, 416, 159–163, 2002.

Guo, Z. T., Sun, B., Zhang, Z. S., Peng, S. Z., Xiao, G. Q., Ge, J. Y., Hao, Q. Z., Qiao, Y. S., Liang, M. Y., Liu, J. F., Yin, Q. Z., and Wei, J. J.: A major reorganization of Asian climate by the early Miocene, Clim. Past, 4, 153–174, doi:10.5194/cp-4-153-2008, 2008.

Sporopollen evidence for Late Miocene stepwise aridification

J. Liu et al.

Title Page

Abstract | Introduction

Conclusions | References

Tables | Figures

|◄ | ►|

◄ | ►

Back | Close

Full Screen / Esc

Printer-friendly Version

Interactive Discussion

Gupta, A. K., Singh, R. K., Joseph, S., and Thomas, E.: Indian Ocean high-productivity event (10–8 Ma): linked to global cooling or to the initiation of the Indian monsoons?, Geology, 32, 753–756, 2004.

Herzschuh, U., Kürschner, H., and Ma, Y. Z.: The surface pollen and relative pollen production of the desert vegetation of the Alashan Plateau, western Inner Mongolia, Chinese Sci. Bull., 48, 1488–1493, 2003.

Huang, D. S.: Vegetation of Gansu Province, Science and Technology of Gansu, Science and Technology of Gansu Press, Lanzhou, 1997.

Huang, Y. S., Clemens, S. C., Liu, W. G., Wang, Y., and Prell, W. L.: Large-scale hydrological change drove the late Miocene C_4 plant expansion in the Himalayan foreland and Arabian Peninsula, Geology, 35, 531–534, 2007.

Hui, Z. C., Li, J. J., Xu, Q. H., Song, C. H., Zhang, J., Wu, F. L., and Zhao, Z. J.: Miocene vegetation and climatic changes reconstructed from a sporopollen record of the Tianshui Basin, NE Tibetan Plateau, Palaeogeogr. Palaeocl., 308, 373–382, 2011.

Jacques, F. M. B., Shi, G., and Wang, W. M.: Neogene zonal vegetation of China and the evolution of the winter monsoon, Bull. Geosci., 88, 175–193, 2013.

Jia, G. D., Peng, P. A., Zhao, Q. H., and Jian, Z. M.: Changes in terrestrial ecosystem since 30 Ma in East Asia: stable isotope evidence from black carbon in the South China Sea, Geology, 31, 1093–1096, 2003.

Kutzbach, J. E., Prell, W. L., and Ruddiman, W. F.: Sensitivity of Eurasian climate to surface uplift of the Tibetan Plateau, J. Geol., 101, 177–190, 1993.

Lease, R. O., Burbank, D. W., Gehrels, G. E., Wang, Z. C., and Yuan, D. Y.: Signatures of mountain building: detrital zircon U/Pb ages from northeastern Tibet, Geology, 35, 239–242, 2007.

Li, J. J.: Uplift of Qinghai-Xizang (Tibet) Plateau and global change, Lanzhou University Press, Lanzhou, China, 1995.

Li, J. J., Feng, Z. D., and Tang, L. Y.: Late Quaternary monsoon patterns on the Loess Plateau of China, Earth Surf. Proc. Land., 13, 125–135, 1988.

Li, J. J., Zhang, J., Song, C. H., Zhao, Z. J., Zhang, Y., and Wang, X. X.: Miocene Bahean stratigraphy in the Longzhong Basin, northern central China and its implications in environmental change, Sci. China Ser. D, 49, 1270–1279, 2006.

Sporopollen evidence for Late Miocene stepwise aridification

J. Liu et al.

Title Page

Abstract | Introduction

Conclusions | References

Tables | Figures

|◄ | ►|

◄ | ►

Back | Close

Full Screen / Esc

Printer-friendly Version

Interactive Discussion

Li, J. J., Fang, X. M., Song, C. H., Pan, B. T., Ma, Y. Z., and Yan, M. D.: Late Miocene–
Quaternary rapid stepwise uplift of the NE Tibetan Plateau and its effects on climatic and
environmental changes, Quaternary Res., 81, 400–423, 2014.

Li, W. Y. and Yao, Z. J.: A study on the quantitative relationship between *Pinus* pollen in surface
sample and *Pinus* vegetation, Chinese Bulletin of Botany, 32, 943–950, 1990.

Li, Y. Y., Zhang, X. S., Zhou, G. S., and Ni, J.: The quantitative relationship between several
common types of surface pollen and vegetation in northern China, Chinese Sci. Bull., 45,
761–765, 2000.

Liu, H. Y., Cui, H. T., Pott, R., and Speier, M.: The surface pollen of the woodland-steppe eco-
tone in southeastern Inner Mongolia, China, Rev. Palaeobot. Palyno., 105, 237–250, 1999.

Liu, L. P., Eronen, J. T., and Fortelius, M.: Significant mid-latitude aridity in the middle Miocene
of East Asia, Palaeogeogr. Palaeocl., 279, 201–206, 2009.

Liu, L. P., Zheng, S. H., Zhang, Z. Q., and Wang, L. H.: Late Miocene–Early Pliocene biostratig-
raphy and Miocene/Pliocene boundary in the Dongwan section, Gansu, Vertebrat. Palasi-
atic., 49, 229–240, 2011.

Liu, X. D. and Yin, Z. Y.: Sensitivity of East Asian monsoon climate to the uplift of the Tibetan
Plateau, Palaeogeogr. Palaeocl., 183, 223–245, 2002.

Liu, Y.-S. C., Utescher, T., Zhou, Z. K., and Sun, B. N.: The evolution of Miocene climates
in North China: preliminary results of quantitative reconstructions from plant fossil records,
Palaeogeogr. Palaeocl., 304, 308–317, 2011.

Ma, Y. Z., Liu, K., Feng, Z. D., Sang, Y. L., Wang, W., and Sun, A. Z.: A survey of modern pollen
and vegetation along a south–north transect in Mongolia, J. Biogeogr., 35, 1512–1532, 2008.

Miao, Y. F., Herrmann, M., Wu, F. L., Yan, X. L., and Yang, S. L.: What controlled Mid–Late
Miocene long-term aridification in Central Asia? – Global cooling or Tibetan Plateau uplift:
a review, Earth-Sci. Rev., 112, 155–172, 2012.

Molnar, P., Boos, W. R., and Battisti, D. S.: Orographic controls on climate and paleoclimate
of Asia: thermal and mechanical roles for the Tibetan Plateau, Annu. Rev. Earth Pl. Sc., 38,
77–102, 2010.

Peng, T. J., Li, J. J., Song, C. H., Zhao, Z. J., Zhang, J., Hui, Z. C., and King, J. W.: Biomarkers
challenge early Miocene loess and inferred Asian desertification, Geophys. Res. Lett., 39,
L06702, doi:06710.01029/02012GL050934, 2012.

Title Page

Abstract | Introduction

Conclusions | References

Tables | Figures

|◀ | ▶|

◀ | ▶

Back | Close

Full Screen / Esc

Printer-friendly Version

Interactive Discussion

Pound, M. J., Haywood, A. M., Salzmann, U., and Riding, J. B.: Global vegetation dynamics and latitudinal temperature gradients during the Mid to Late Miocene (15.97–5.33 Ma), Earth-Sci. Rev., 112, 1–22, 2012.

Qiang, X. K., An, Z. S., Song, Y. G., Chang, H., Sun, Y. B., Liu, W. G., Ao, H., Dong, J. B., Fu, C. F., and Wu, F.: New eolian red clay sequence on the western Chinese Loess Plateau linked to onset of Asian desertification about 25 Ma ago, Sci. China Ser. D, 54, 136–144, 2011.

Qin, A. L., Wang, M. M., Cun, Y. Z., Yang, F. S., Wang, S. S., Ran, J. H., and Wang, X. Q.: Phylogeographic evidence for a link of species divergence of *Ephedra* in the Qinghai-Tibetan Plateau and adjacent regions to the Miocene Asian aridification, PLOS One, 8, e56243, doi:10.1371/journal.pone.0056243, 2013.

Quade, J., Cerling, T. E., and Bowman, J. R.: Development of Asian monsoon revealed by marked ecological shift during the latest Miocene in northern Pakistan, Nature, 342, 163–166, 1989.

Shi, C. M., Ji, Y. J., Liu, L., Wang, L., and Zhang, D. X.: Impact of climate changes from Middle Miocene onwards on evolutionary diversification in Eurasia: insights from the mesobuthid scorpions, Mol. Ecol., 22, 1700–1716, 2013.

Song, Z. C.: Early Tertiary Sporopollen in Bohai Coastal Areas, Science Press, Beijing, China, 1978.

Song, Z. C.: Fossil Spores and Pollen of China: the Late Cretaceous and Tertiary Spores and Pollen, Science Press, Beijing, China, 1999.

Steinke, S., Groeneveld, J., Johnstone, H., and Rendle-Bühring, R.: East Asian summer monsoon weakening after 7.5 Ma: evidence from combined planktonic foraminifera Mg/Ca and δ^{18}O (ODP Site 1146; northern South China Sea), Palaeogeogr. Palaeocl., 289, 33–43, 2010.

Sun, J. M., Ye, J., Wu, W. Y., Ni, X. J., Bi, S. D., Zhang, Z. Q., Liu, W. M., and Meng, J.: Late Oligocene–Miocene mid-latitude aridification and wind patterns in the Asian interior, Geology, 38, 515–518, 2010.

Sun, X. J. and Wang, P. X.: How old is the Asian monsoon system? – Palaeobotanical records from China, Palaeogeogr. Palaeocl., 222, 181–222, 2005.

Tapponnier, P., Xu, Z. Q., Roger, F., Meyer, B., Arnaud, N., Wittlinger, G., and Yang, J. S.: Oblique stepwise rise and growth of the Tibet Plateau, Science, 294, 1671–1677, 2001.

Tong, G. B., Yang, X. D., Wang, S. M., and Xia, L. H.: Sporo-pollen dissemination and quantitative character of surface sample of Manzhouli-Dayangshu region, Acta Bot. Sin., 38, 814–821, 1995.

van Dam, J. A.: Geographic and temporal patterns in the late Neogene (12–3 Ma) aridification of Europe: the use of small mammals as paleoprecipitation proxies, Palaeogeogr. Palaeocl., 238, 190–218, 2006.

Wan, S. M., Clift, P. D., Li, A. C., Li, T. G., and Yin, X. B.: Geochemical records in the South China Sea: implications for East Asian summer monsoon evolution over the last 20 Ma, Geol. Soc. Sp., 342, 245–263, 2010.

Wang, F. X.: Pollen Flora of China, Science Press, Beijing, China, 1995.

Wang, X. M., Qiu, Z. D., Li, Q., Wang, B. Y., Qiu, Z. X., Downs, W. R., Xie, G. P., Xie, J. Y., Deng, T., Takeuchi, G. T., Tseng, Z. J., Chang, M., Liu, J., Wang, Y., Biasatti, D., Sun, Z. C., Fang, X. M., and Meng, Q. Q.: Vertebrate paleontology, biostratigraphy, geochronology, and paleoenvironment of Qaidam Basin in northern Tibetan Plateau, Palaeogeogr. Palaeocl., 254, 363–385, 2007.

Wang, X. X., Li, J. J., Song, C. H., Zattin, M., Zhao, Z. J., Zhang, J., Zhang, Y., and He, K.: Late Cenozoic orogenic history of Western Qinling inferred from sedimentation of Tianshui basin, northeastern margin of Tibetan Plateau, Int. J. Earth Sci., 101, 1345–1356, 2012.

Wang, Y. and Deng, T.: A 25 myr isotopic record of paleodiet and environmental change from fossil mammals and paleosols from the NE margin of the Tibetan Plateau, Earth Planet. Sc. Lett., 236, 322–338, 2005.

Wang, Y., Deng, T., and Biasatti, D.: Ancient diets indicate significant uplift of southern Tibet after ca. 7 Ma, Geology, 34, 309–312, 2006.

Wang, Y. L., Fang, X. M., Zhang, T. W., Li, Y. M., Wu, Y. Q., He, D. X., and Gao, Y.: Distribution of biomarkers in lacustrine sediments of the Linxia Basin, NE Tibetan Plateau, NW China: significance for climate change, Sediment. Geol., 243, 108–116, 2012.

Zachos, J., Pagani, M., Sloan, L., Thomas, E., and Billups, K.: Trends, rhythms, and aberrations in global climate 65 Ma to present, Science, 292, 686–693, 2001.

Zhang, C. F., Wang, Y., Deng, T., Wang, X. M., Biasatti, D., Xu, Y. F., and Li, Q.: C_4 expansion in the central Inner Mongolia during the latest Miocene and early Pliocene, Earth Planet. Sc. Lett., 287, 311–319, 2009.

Sporopollen evidence for Late Miocene stepwise aridification

J. Liu et al.

Title Page

Abstract | Introduction

Conclusions | References

Tables | Figures

Back | Close

Full Screen / Esc

Printer-friendly Version

Interactive Discussion

Zhang, C. F., Wang, Y., Li, Q., Wang, X. M., Deng, T., Tseng, Z. J., Takeuchi, G. T., Xie, G. P., and Xu, Y. F.: Diets and environments of late Cenozoic mammals in the Qaidam Basin, Tibetan Plateau: evidence from stable isotopes, Earth Planet. Sc. Lett., 333, 70–82, 2012.

Zhang, J., Li, J. J., Song, C. H., Zhao, Z. J., Xie, G. P., Wang, X. X., Hui, Z. C., and Peng, T. J.: Paleomagnetic ages of Miocene fluvio-lacustrine sediments in the Tianshui Basin, western China, J. Asian Earth Sci., 62, 341–348, 2013.

Zhang, M. L. and Fritsch, P. W.: Evolutionary response of *Caragana* (Fabaceae) to Qinghai-Tibetan Plateau uplift and Asian interior aridification, Plant Syst. Evol., 288, 191–199, 2010.

Zhang, Z. Q.: Chinese Late Neogene land mammal community and the environmental changes of East Asia, Vertebrat. Palasiatic., 44, 133–142, 2006.

Zheng, D. W., Zhang, P. Z., Wan, J. L., Yuan, D. Y., Li, C. Y., Yin, G. M., Zhang, G. L., Wang, Z. C., Min, W., and Chen, J.: Rapid exhumation at ∼ 8 Ma on the Liupan Shan thrust fault from apatite fission-track thermochronology: implications for growth of the northeastern Tibetan Plateau margin, Earth Planet. Sc. Lett., 248, 198–208, 2006.

Zheng, D. W., Clark, M. K., Zhang, P. Z., Zheng, W. J., and Farley, K. A.: Erosion, fault initiation and topographic growth of the North Qilian Shan (northern Tibetan Plateau), Geosphere, 6, 937–941, 2010.

Sporopollen evidence for Late Miocene stepwise aridification

J. Liu et al.

Title Page

Abstract | Introduction

Conclusions | References

Tables | Figures

|◄ | ►|

◄ | ►

Back | Close

Full Screen / Esc

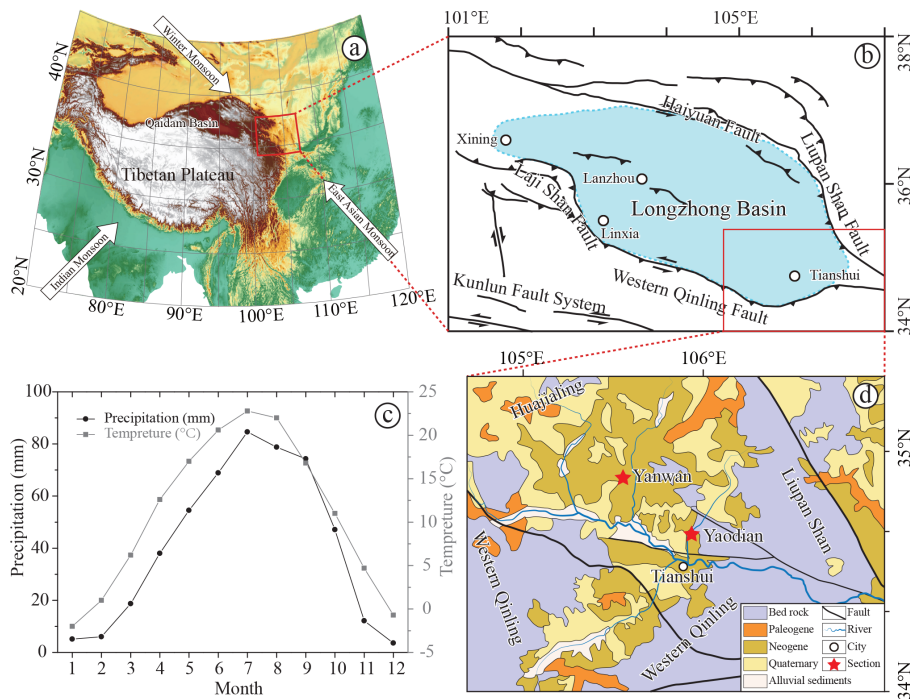Printer-friendly Version

Interactive Discussion

Figure 1. Geographic setting of Yaodian Section. **(a)** The location of the Longzhong Basin. **(b)** The major tectonic faults of the Longzhong Basin. **(c)** Mean monthly temperature and mean monthly precipitation between in the Tianshui area, 1971–2000. **(d)** Geological map of the Tianshui Basin.
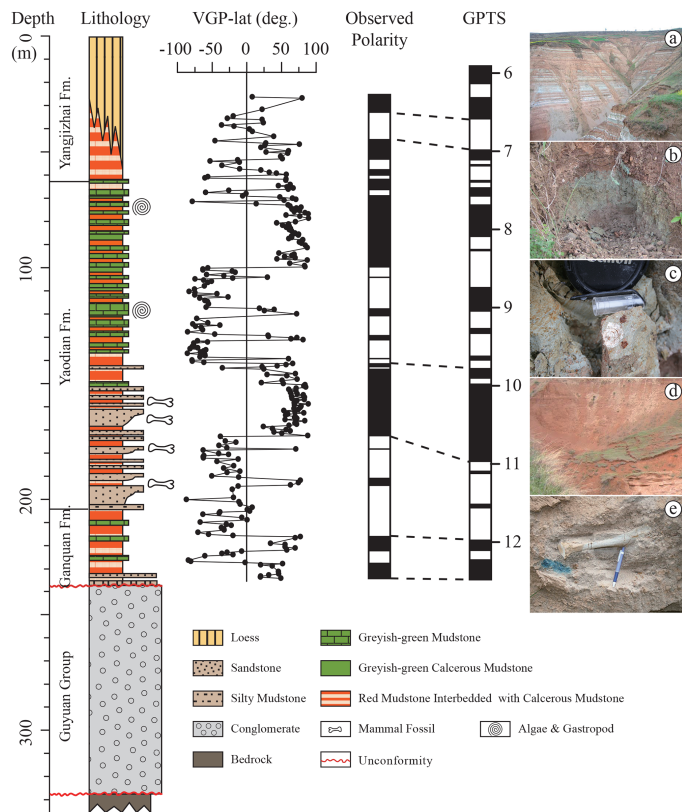
Figure 2. Lithology and magnetic stratigraphy of the Yaodian Section (according to Li et al., 2006, 2007). **(a)** The entire Yaodian Fm **(b)** Yangjizhai Fm distal floodplain to palustrine deposits **(c)** Yaodian Fm upper stratum lacustrine deposits, containing gastropod fossil fragments. **(d)** Yaodian Fm middle stratum floodplain deposits, with paleosols. **(e)** Yaodian Fm lower stratum fluvial channel deposits, containing fossilized animal bones.
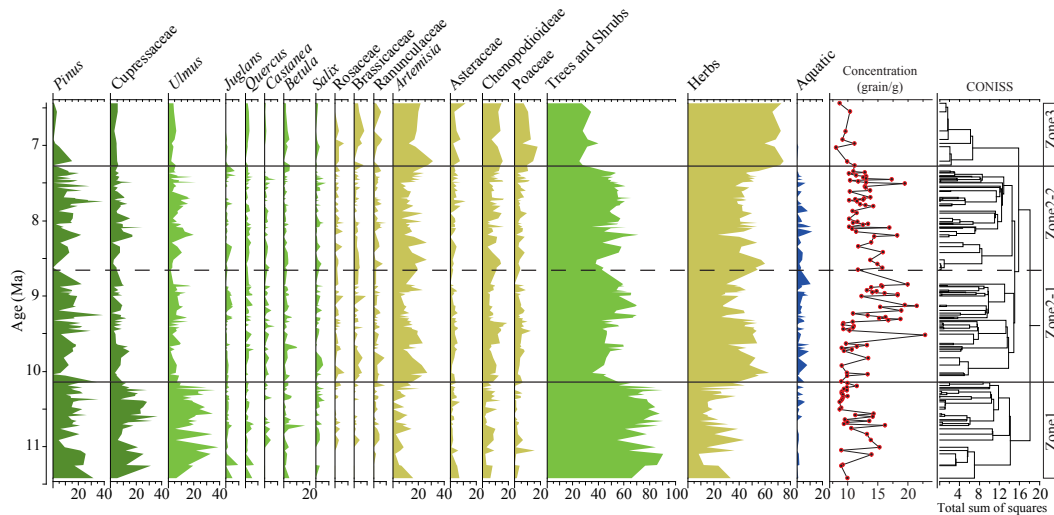
Figure 3. Histogram showing sporopollen percentages for the most significant angiosperms and gymnosperms.

Sporopollen evidence for Late Miocene stepwise aridification

J. Liu et al.

Drier Drier Drier Drier Drier Drier Drier

Ice sheet-volume increase

Northern Hemisphere Ice-sheets

Southern Hemisphere Ice-sheets

Age (Ma)

7 8 9 10 11

20 40 60 80	50 100 150	50 100		0 10 20	0 1 2	-34 -28 -24	2 3 4	
Herbs (%)	Susceptibility (10⁻⁸m³·kg⁻¹)	Astermisia (%)	Herbivorous mammal species	MAR (10-40 µm)	δ¹⁸O_seawater	δ¹³C (C₃₁ n-Alkane. ‰)	δ¹⁸O (PBD,‰)	Major uplift

Herbs (%)
Yaodian Section
a

Susceptibility
$(10^{-8}m^3 \cdot kg^{-1})$
Yaodian Section
b

Astermisia (%)
Yanwan Section
c

Herbivorous mammal species
Tianshui Basin
d

MAR
(10-40 µm)
Linxia Basin
e

$\delta^{18}O_{seawater}$
ODP Site 1146
f

$\delta^{13}C$
(C_{31} n-Alkane. ‰)
ODP Site 722
g

$\delta^{18}O$
(PBD,‰)
Global Deep Sea
h

Major uplift
Tibetan Plateau
i

Figure 4. Proxy records of aridification for East Asia during the Late Miocene. **(a)** Herbaceous pollen contents (%) for the Yaodian Section (this study); **(b)** Yaodian Section magnetic susceptibility (this study); **(c)** Drought-tolerant *Artemisia* pollen content (%) for the Yanwan Section, northern Tianshui Basin (Hui et al., 2011); **(d)** Herbivorous mammal species in the Tianshui Basin (Guo et al., 2002; Li et al., 2006; Zhang et al., 2013; L. P. Liu et al., 2011). Black circles represent species which adapt to relatively arid environment, including *Sinocricetus zdanskyi*, *Kowalskia* sp., *Hansdebmijnia pusillus*, *Lophocricetus grabaui*, *Mesosiphneus praetingi*, *M.* sp., *Paralactaga anderssoni*, *Parasoriculus* sp., *Prosiphneus eriksoni*, *P. licenti*, *P. tianzuensis*, *Prospermophilus orientalis*, *Pseudomeriones abbreuuuus*, *P. complicidens*, Sciuridae, *Sicista* sp., *Alilepus annectens*, *Allorattus* sp., *Apodemus* sp., *Chardina* n. sp., *C. sinensis*, *C. truncatus*, *Chardinomys nihowanicus*, *C.* sp., *C. yusheensis*, *Pliosiphneus lyratus*, *Cricetinus mesolophidus*, *Mimomys teilhardi*, *Paenepetenyia zhudingi*, *Sinotamias* sp., *Ochotona gracilis*, *O. lagreli*, *O. lingtaica*, *O. minor*, *O. plicodenta*, *O.* sp., *Ochotonoma* sp., *O. primitiva*, *Trischizolagus mirificus*, *Hipparion chiai*, *H. dermatorhinum*, *H. fossatum*, *H. plocodus*, *H.* sp., *H. weihoense*, and *Gazella* sp.; grey triangles represent species which adapt to relatively humid environment, including *Chleuastochoerus stehlini*, *Cervavitus novorossiae*, Cervidae gen. et sp. Indet., *Palaeotragus microdon*, *P.* sp., *Samotherium sinense*, *S.* sp., Rhinocerotidae indet., *Acerorhinus fuguebsis*, *Chilotherium habereri*, *C.* sp., *C. wimani* and *Protanancus tobieni*. **(e)** Eolian sediment mass accumulation rates for the Linxia Basin, northeastern TP (Fan et al., 2006); **(f)** South China Sea $\delta^{18}O_{seawater}$ estimates from ODP Site 1146 (Steinke et al., 2010); **(g)** Compiled global deep-sea $\delta^{18}O$ values (Zachos et al., 2001); **(h)** Schematic model showing major periods of TP uplift (Molnar et al., 2010; Fang et al., 2003, 2005; Li et al., 2014; Enkelmann et al., 2006; Zheng et al., 2006, 2010; Wang et al., 2012, 2006; Lease et al., 2007).